CANADIAN JOURNAL OF RESEARCH

VOLUME 19 JUNE, 1941 NUMBER 6

CONTENTS

NATIONAL RESEARCH COUNCIL
OTTAWA, CANADA

Publications and Subscriptions

The Canadian Journal of Research is issued monthly in four sections, as follows:

A. Physical Sciences
B. Chemical Sciences
C. Botanical Sciences
D. Zoological Sciences

For the present, Sections A and B are issued under a single cover, as also are Sections C and D, with separate pagination of the four sections, to permit separate binding, if desired.

Subscription rates, postage paid to any part of the world (effective 1 April, 1939), are as follows:

	Annual	*Single Copy*
A and B	$ 2.50	$ 0.50
C and D	2.50	0.50
Four sections, complete	4.00	—

The Canadian Journal of Research is published by the National Research Council of Canada under authority of the Chairman of the Committee of the Privy Council on Scientific and Industrial Research. All correspondence should be addressed:

National Research Council, Ottawa, Canada.

Notice to Contributors

Fifty reprints of each paper are supplied free. Additional reprints, if required, will be supplied according to a prescribed schedule of charges.

Canadian Journal of Research

Issued by THE NATIONAL RESEARCH COUNCIL OF CANADA

VOL. 19, SEC. A. JUNE, 1941 NUMBER 6

RECOMPRESSION PHENOMENA IN STEAM NOZZLES

PART II[1]

BY CHARLES ALEXANDER ROBB

IV. Discussion of Experimental Data

(a) Types of Recompression in the Final Series of Tests

The objective at this point in the program was to find what laws, if any, govern recompression. Mellanby and Kerr, in their paper on pressure flow in steam nozzles (7, p. 125), say of recompression, "It would appear that a recompression may be either of wave form or continuous; and such alternatives, taken in conjunction with the almost invariable pressure fluctuations that exist might seem to indicate that a recompression follows no laws but those of chance."

Inspection of the expansion curves for nozzle No. 8 (Fig. 21) shows a dip marked *A* at scale reading 2 in. due to the vena contracta effect, and the recovery or contracta recompression amounts to $2\frac{1}{2}$ psi. The vena contracta appears in some degree at each of the back pressures including the 43 psi gauge. It was proposed to eliminate the dip *A* by adjusting the inlet radius of the nozzle to reduce the necking down of the jet. The results are shown for nozzle No. 9 in Fig. 22 and for nozzle No. 10 in Fig. 23 in which the dip has almost entirely disappeared.

With the same nozzle, No. 8, an additional break or notch is noted at *B* in Fig. 21 at scale reading 2.8 in. This notch appears in the region where supersaturation, as described by Stodola (11), Goudie (3), Powell (9), and others (1, 10, 12-14), may be expected. Considering the process to be isentropic, the notch occurs in the wet region of the Mollier diagram, below the saturation line and in the region of the Wilson line or zone. The observation of this notch and consideration of the latent recompression that characterizes the pressure disturbance was at the time of these experiments (1931–2) a novel contribution of this investigation, and further reference will be made to this interesting phenomenon.

When the notch was first noted, the author was disposed to attribute it to a roughness in the surface of the nozzle. The persistence of the notch in the same region in various nozzles that were known to be free from rough spots, and at various inlet pressures, made it necessary to look elsewhere for the cause. Later experiments, by other investigators (1, 10, 12–14) using a modified technique, have proved the notch of the author's pressure expansion

[1] *Part I appeared in the May issue.*

curves to be due to change of state of the steam. The latent heat, being suddenly released as the supersaturated steam condenses, becomes available to accelerate the stream or jet. The formation of the drops tends to obstruct the flow since the drops will tend to lag behind the stream, and, failing accelera-

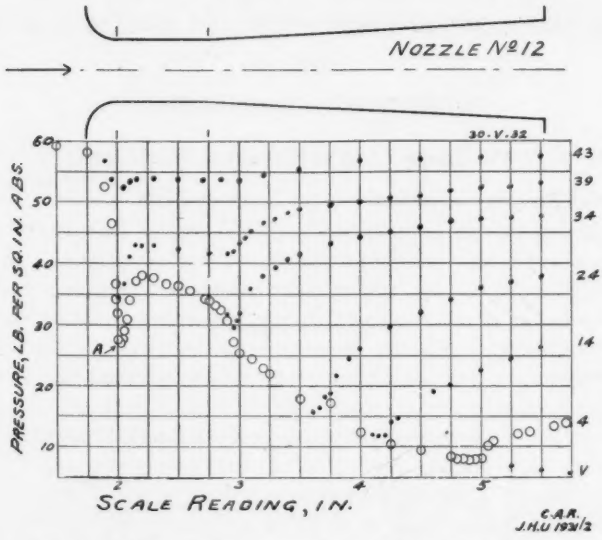

FIG. 25. *Vena contracta recompression in brass nozzle No. 12.*

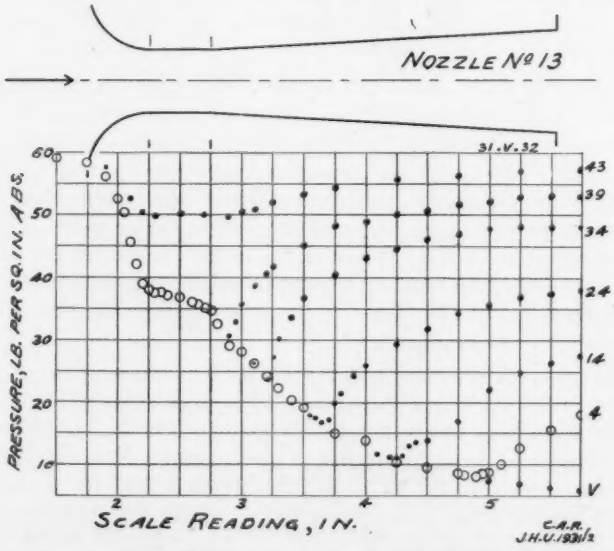

FIG. 26. *Equilibrium recompression in brass nozzle No. 13.*

tion of the jet, the heat will tend to expand the steam. This change in volume is resisted by the nozzle walls, with the result that the static pressure builds up, and this increase of pressure, or what is described above as latent recompression, occurs. The amount of the pressure increase was observed by

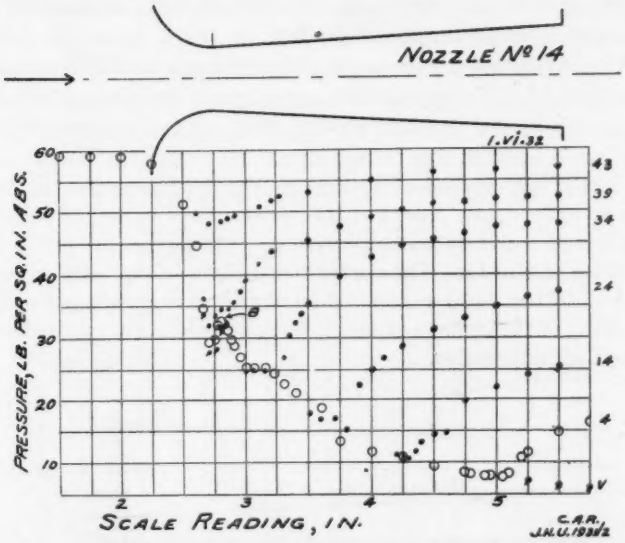

FIG. 27. *The "notch" at B, due to latent recompression in brass nozzle No. 14.*

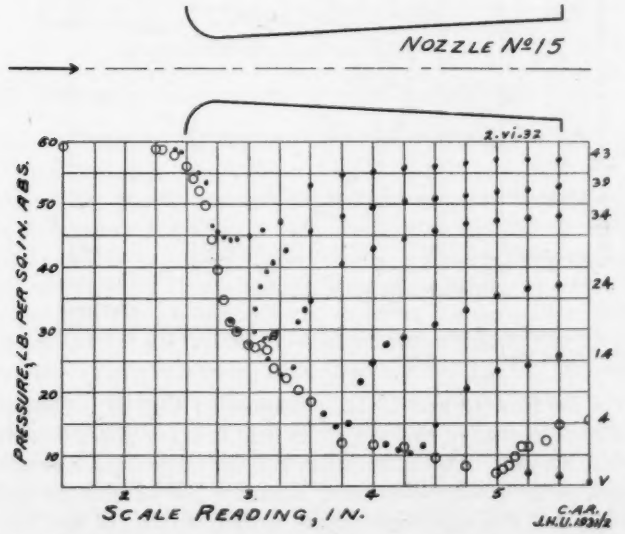

FIG. 28. *Latent recompression in brass nozzle No. 15 at scale reading 3.*

means of the search tube and pressure gauge. The notch is repeated in the various expansion curves of Fig. 21 for nozzle No. 8 and the coincidence of the 14 psi gauge back pressure observations with the 4 psi curve is recorded.

The effect of changing the inlet radius and the length of the parallel section or throat on the rate of expansion can be observed in the slope of the pressure expansion curves for the nozzles Nos. 8 to 11 (Figs. 21 to 24). The slope progressively increases as the throat is shortened and the radius reduced.

In the final series of tests, which were made on the polished drawn brass nozzles Nos. 12, 13, 14, and 15, the dip indicating vena contracta recompression is noted at *A* in Fig. 25 for nozzle No. 12. The notch marked *B*, indicating latent recompression, appears in Fig. 27 for nozzle No. 14 and in the other curves for nozzle No. 14 at inlet pressures of 15 and 30 psi gauge and back pressures of 5 and 14 psi respectively. The dip occurs in the low inlet pressure curves of No. 12. The curves resulting from the tests on Nos. 12 to 15, Figs. 25 to 28, can be superimposed on one another in such a way that they show the effects of the changes in nozzle form on the rate of expansion, change of state, and recompression.

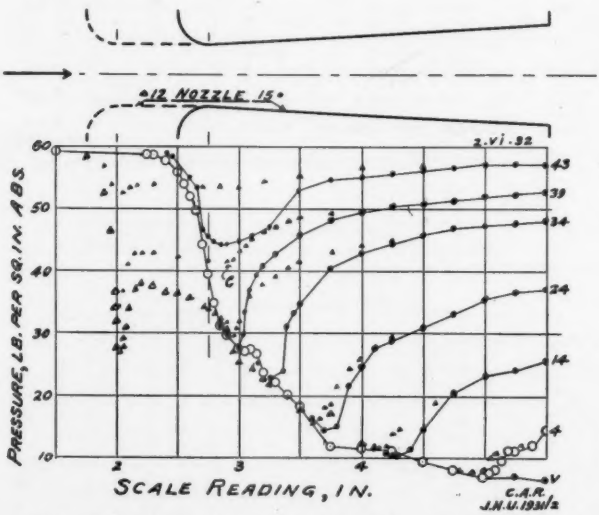

FIG. 29. *Elimination of vena contracta "dip" by shortening of throat (No. 15) despite small inlet radius ($\frac{1}{4}$ in.).*

The curves for Nos. 12 and 15 are combined in Fig. 29. They show the effect of the parallel part or throat $\frac{3}{4}$ in. in length, other dimensions being the same for both nozzles. The inlet radius is $\frac{1}{4}$ in. The vena contracta effect and vena contracta recompression occur in nozzle No. 12 with the long throat only. Equilibrium recompression occurs earlier in No. 12 but the recompression pressure, p_r, is higher; that is to say, the steam does not expand to

such a low pressure in nozzle No. 12. The difference in p_r is greater at pressures above the critical, as for example at C in Fig. 29. The symbol p_r is used here to indicate the lowest static pressure attained by the steam in the nozzle as shown by the pressure expansion curve. With particular reference to recompression phenomena, p_r indicates the base of the cusp in the whole pressure expansion curve at which the pressure changes from a decreasing to an increasing value, that is to say, the steam ceases to expand and begins to recompress. The recompression curves occur earlier or the recompression pressures, p_r, are reached earlier in the case of nozzle No. 12, although ultimately the expansion curves coincide, with no apparent loss of pressure.

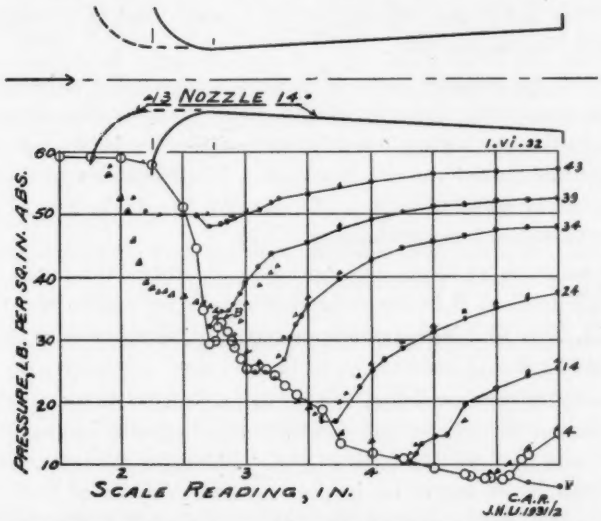

FIG. 30. *Expansion curve and shortened throat for large inlet radius ($\frac{1}{2}$ in.).*

The curves for nozzles Nos. 13 and 14 are combined in Fig. 30. The throat length or parallel part is reduced from $\frac{3}{4}$ in. in No. 13 to zero in No. 14. The inlet radius ($\frac{1}{2}$ in.) is common to both. The vena contracta effect and contracta recompression are absent from each, and the latent recompression survives only in the curves for nozzle No. 14. The resulting notch is shown at B. An important difference in the rate of expansion is noted, the curve being steeper and the expansion more rapid in the curves for nozzle No. 14 than in those for No. 13. Similarly the curves for nozzle No. 15 are steeper and show a more rapid expansion than those for No. 12 (Fig. 29). In Fig. 30 the equilibrium recompression occurs earlier for No. 13, the nozzle with the $\frac{3}{4}$ in. parallel section, than it does for No. 14, with the exception of the 39 lb. curve. In the latter case the situation is reversed, the expansion in nozzle No. 14 is earlier, and the value of the recompression pressure p_r is slightly higher. The point of equilibrium recompression coincides approximately with the point of latent recompression, that is, the notch.

When the expansion curves for nozzle No. 14 (Fig. 27) are superimposed on those for No. 15 (Fig. 28), the inlet radius contributes the only change in the nozzle form. The equilibrium recompression in nozzle No. 14 is consistently earlier than in No. 15. Equilibrium recompression on the 39 psi curve for nozzle No. 14 coincides with the notch, and the recompression pressure p_r of nozzle No. 14 is higher, showing less complete expansion than No. 15.

It is noted that the notch appears in each of the curves for nozzles Nos. 8 to 11 shown in Figs. 21 to 24, whereas in the final series with nozzles Nos. 12 to 15 the step appears only in the case of nozzle No. 14, Fig. 27, and No. 15, Fig. 28. The notch and dip appear at a scale reading of approximately 2.75 in. and 3 in. respectively.

Examples of the peculiar forms of expansion curves due to harmonic vibrations can be seen in Fig. 23 for nozzle No. 10. The wave-like vibrations occur in the jets having the higher velocities such as Curves 14, 4, and V, and only after the jet has passed the nozzle mouth. The frequency of the vibrations increases with the speed of the jet. In test No. 10—45/V, Fig. 23, the amplitude of the vibration is approximately 0.7 in.

The phenomenon of latent recompression results in the notch referred to above and is marked *B* in the expansion curves for nozzle No. 14, Fig. 27, and No. 15, Fig. 28. The amount of recompression involved in the notch of No. 14 is 3½ psi.

The possibility that erosion of the jet surface might disturb the continuity of the expansion curves received special consideration in connection with the tests of the cast-iron nozzles, Nos. 8 to 11. Following the tests, nozzle No. 11 was cut through the centre for inspection, and evidence of both blow holes and erosion was found. Considering the short time that the nozzles were in service, the erosion appeared severe. It resembled cavitation resulting from a continued bombardment of collapsing bubbles or drops. The erosion was most severe in the region where the jet left the throat and entered the diverging part of the nozzle. A comparison of the curves for nozzles Nos. 8 to 11 with those of Nos. 12 to 15 would suggest that since the notch appears in all the curves for the cast-iron channels, Nos. 8 to 11 (Figs. 21 to 24) but in the case of the brass nozzles it appears in the curves of No. 14 and No. 15 only, possibly the notch in the curves of nozzles Nos. 8 and 9 is due to shock recompression resulting from the erosion or pitting.

In connection with the phenomenon of latent recompression and the notch in the pressure expansion curve which was observed at this time and has been described, it should be noted that these tests are the first of a series. At the time of the tests, certain facts were obscure, and they were investigated by means of a modified technique, of which the parallel or extended throat used in these tests formed a part. Later work by other investigators made clear certain factors such as the growth of the water drops (10, 13).

(b) Recompression Effects and Angle of Flare

A comparison of these effects in nozzles having small and large angles of flare can be made by means of the tests of nozzles Nos. 14 and 15 (Figs. 27 and 28) and nozzle No. 6 (Fig. 19). In the latter the flare or nozzle angle is 12°, and the expansion to about atmospheric pressure takes place with great rapidity. The equilibrium recompression is almost as rapid and results in a sharp cusp in the expansion curves for the higher back pressures. The small radius of the inlet or converging section contributes to the rapid expansion, which for moderate pressure ranges demands a short nozzle only, and the combination of the small inlet radius and large angle of flare tends to limit the freedom of control for experimental work in the region where phenomena involving change of state, and recompression, occur. The larger inlet radius of $\frac{1}{2}$ in. in the case of nozzle No. 14, Fig. 27, and $\frac{1}{4}$ in. in No. 15, Fig. 28, in combination with the parallel section or throat and the smaller angle of flare of 6 degrees, tends to slow down the rate of expansion and makes it possible to observe pressure values at measurable intervals along the axis, as shown in the curves of Figs. 25 to 31.

(c) Prevention of Recompression

To avoid recompression, the design of the nozzle and operating conditions must be considered with a view to avoiding each specific type of recompression.

Equilibrium recompression must be expected wherever the nozzle takes the converging-diverging form and the outlet or back pressure is raised above a specified minimum; the behaviour of this type of recompression will depend upon the angle of flare of the diverging section. The effect of the angle of flare is shown also by a comparison of the curves for nozzle No. 6, Fig. 19, with those for nozzle No. 13, Fig. 26.

Latent recompression has been avoided by reducing the rate of expansion of the steam in the nozzle as in No. 13. Flow tests summarized in Table V and later experiments by other investigators (10) have shown that the means described of reducing the rate of expansion are undesirable. The later experiments have shown that preliminary condensation with rapid growth of drop size occurs when the rate of expansion is decreased. Large drops cause blade erosion. Hence this cure for latent recompression is not satisfactory. It would seem better to allow it to occur, as supersaturation persists.

Vena contracta recompression can be avoided by the use of a liberal inlet radius, with or without a short throat in which the length is from zero to not more than the throat diameter. Examples in which this type of recompression has been eliminated are to be found in nozzles Nos. 13 to 15, for which the pressure expansion curves are shown in Figs. 26 to 28. The later tests referred to above have shown that no length of straight throat is desirable or necessary (10).

Recompression due to roughness of the nozzle surface has been avoided in the case of the cast-iron nozzle No. 9 by substituting the polished drawn

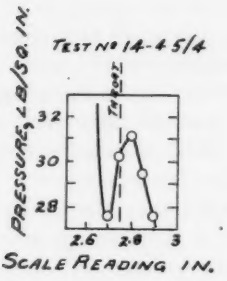

FIG. 31. *Notch produced by latent recompression in No. 14.*

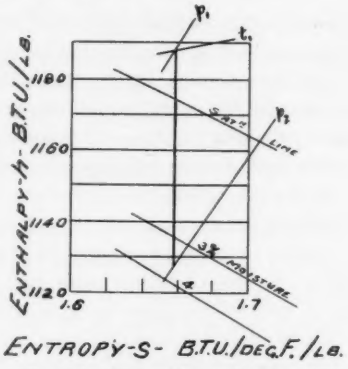

FIG. 32. *Saturation and supersaturation lines in the Mollier diagram.*

brass nozzle No. 13, as will be seen by comparing the respective curves of Figs. 22 and 26.

The notch in the expansion curve representing the test with nozzle No. 14—45/4, as shown at *B*, in Fig. 27, is reproduced on a large scale in Fig. 31. Its position corresponds to a region near the throat of the nozzle. The valley of the expansion curve is reached immediately before the stream enters, and the following recompression immediately after it leaves the throat. In dealing with the quality of the steam and the change of state, the assumption is made that the expansion through the throat is isentropic. There are losses, but those due to wall friction, eddy currents, and the like, occur mainly after the throat has been passed. The operating conditions for test No. 14—45/4 are shown in the Mollier diagram, Fig. 32. The valley of the notch is seen to be between the 3 and 4% constant moisture lines.

V. Calculation of the Recompression Pressure in a Converging-diverging Nozzle

Some deductions may now be drawn from the results obtained in these experiments. The observed notch and the amount of latent recompression resulting is shown in Fig. 31 for test No. 14—45/4. The effect of the inlet pressure on latent recompression is indicated in Fig. 33, i.e., the latent recompression pressure or height of notch from valley to crest at typical back pressures of tests on nozzle No. 14 (Fig. 27) are plotted as ordinates, and the corresponding inlet pressures, as abscissae. At constant inlet pressure, the lower back pressures on the nozzle tend to a slightly higher latent recompression or notch. For an initial pressure of 59.2 psi abs. recompression at the notch is $3\frac{1}{2}$, $3\frac{1}{4}$, 3, and 3 psi respectively for the back pressures of vacuum, 4, 14, and 24 psi gauge.

The possibility of predicting values of the pressure at which equilibrium recompression will occur in a conventional type of convergent-divergent nozzle

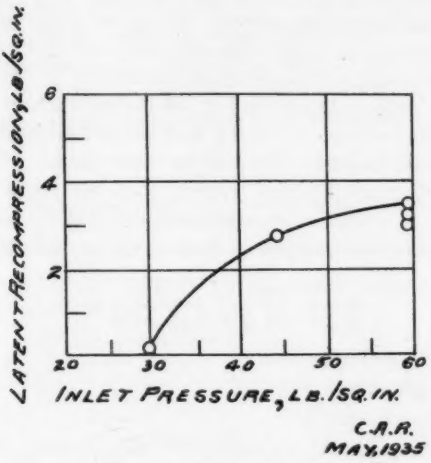

FIG. 33. *Height of notch.*

will now be discussed. Referring to the curves for nozzles Nos. 14 and 15 (Figs. 27 and 28), it will be seen that as the outlet or back pressure is decreased, the steam continues to expand and Curve V, for example, represents a continuous expansion with the notch as the only disturbing element in the continuity. As the outlet pressure is raised, however, there is a halt in the expansion curve and the pressure, which has been decreasing, begins to increase. For example, at a back pressure of 4 psi gauge, the expansion stops and the pressure begins to increase, or equilibrium recompression begins at a scale reading of 5 in. Similarly at a back pressure of 14 psi, recompression begins at a scale reading of 4.25 in., and for 24 psi, at 3.75 in., and so on. It is understood, of course, that the diverging portion of the nozzle must have sufficient length to permit the complete expansion of the steam at the lowest back pressure to which it is proposed to subject the nozzle. It may be useful, in studying the behaviour of a nozzle of this type, to be able to predict the point in the nozzle at which this reversal of pressure or equilibrium recompression will take place, or, since the fundamental Curve 4 can be drawn with a fair degree of accuracy from steam table data for steam in equilibrium with the moisture that it contains, it will be sufficient if one is able to predict the pressure at which the expansion will halt and equilibrium recompression will begin. This pressure, p_r, at which equilibrium recompression begins, will be called simply the recompression pressure in what follows.

The procedure adopted was to investigate the value of p_r relative to $p_1 - p_0$, the difference between the inlet and outlet pressures for various values of p_0 and in the same general type of nozzle. Values of $p_1 - p_0$ for the various tests on nozzles Nos. 12, 13, 14, and 15 were plotted as ordinates against observed values of p_r as abscissae. A curve to approximate all these values was drawn, in view of the possibility that this curve might serve to predict

the value of the recompression pressure, p_r, to be expected in steam nozzles of the convergent-divergent type when the inlet and discharge pressures were known and for variations in the operating conditions in any particular nozzle of this type. The curve is shown in Fig. 34 in conjunction with the observed values of p_r, for nozzles Nos. 12, 13, 14, and 15, including the various pressure conditions of the tests listed in Table II for each nozzle. The approximation is fairly satisfactory, and it would appear that the recompression pressure, p_r, is a function of $p_1 - p_0$. To express the relation between p_r and $p_1 - p_0$ the following equation was computed, from the observed data, by the method of Legendre (5)

$$p_r = \frac{p_1}{59.2}\sqrt{\left(\frac{476}{p_1 - p_0}\right)^3}.$$

where p_r = recompression pressure,
p_1 = inlet pressure,
p_0 = outlet pressure,
$p_1 - p_0$ may be considered to represent the driving force or potential of the flow.

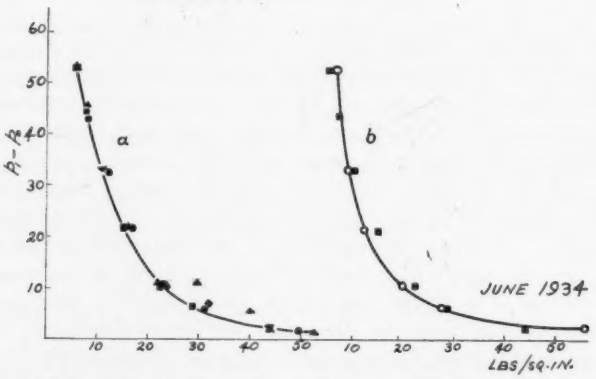

FIG. 34. *(a) Recompression pressures and pressure differences (Nozzle No. 12, ▲; No. 13, ▼; No. 14, ●; No. 15, ■).*
(b) Comparison of the equation for recompression pressures (○, computed points; ■, observed values for No. 15).

Applying the formula to the conditions in nozzle No. 12 operating at an inlet pressure of 59.2 psi abs. and a back pressure of 24 psi gauge, $p_1 - p_2 = 59.2 - (24 + 14.7) = 20.5$. The formula gives a value $p_r = 15.6$ psi abs., which agrees with the observed value. The observed value of p_r from test No. 14—45/24 (Fig. 27) is 15 psi abs., which is the largest variation from the curve for all four nozzles Nos. 12, 13, 14, and 15, operating at a back pressure of 24 psi abs. The value of p_r for the various back pressures in the test on nozzle No. 15 are plotted in Fig. 34, in which the curve is repeated, and the agreement between the estimated and observed values is seen to be good.

In order to test the efficiency of the curve and equation, the method has been applied to published data for convergent-divergent steam nozzles tested by

other investigators, and the following comparison is given of the observed recompression pressure, p_r, and the author's estimated value for p_r.

Mellanby and Kerr (7, p. 125) present a series of pressure expansion curves for various outlet pressures, the initial conditions being 76 psi abs. and 250° F. Table III shows the outlet pressures and the observed and estimated values of p_r.

TABLE III

COMPARISON OF OBSERVED AND ESTIMATED VALUES OF RECOMPRESSION PRESSURE, p_r. INLET PRESSURE, 76 PSI

Outlet pressure psi abs.	Observed recompression pressure, p_r, psi abs., Mellanby and Kerr	Estimated value of p_r, Robb	Difference in per cent of inlet pressure (76 psi)
16.4	15.2	9	8.2
32.7	17.5	13.2	5.7
44.1	21.3	17.9	4.5
54.7	25.8	24	2.4

Stodola (11, p. 83) presents a similar series of pressure expansion curves for which the inlet conditions are 147 psi abs. and 381 to 392° F. Table IV shows a comparison similar to that given above.

TABLE IV

COMPARISON OF OBSERVED AND ESTIMATED VALUES OF RECOMPRESSION, p_r

Outlet pressure	Observed recompression pressure, p_r, psi abs. Stodola	Estimated value of p_r, Robb	Difference in per cent of inlet pressure (147 psi)
144	131	134	2
139	105	102	2
129	66	67	0.7
107	45	47.1	1.4
91	37	37.2	0.13
65	21	27.3	4.3
44	15	20.6	3.8
27	9	16.4	5
12	5	12.7	5.2
8	4	11.9	5.4

The average difference, in percentage of the inlet pressure, between the observed values of the recompression pressure, p_r, and the values estimated by means of the curve and equation, is just more than 5% for the data considered in Table III and 3% for that of Table IV. The examples are taken at random from the reports of representative investigators and would seem

to indicate a fair degree of accuracy for purposes of estimation, and they set limits for the method. The application of the method has been limited to the convergent-divergent type of steam nozzle.

VI. Losses in Nozzles

The ideal expansion of steam in a nozzle is adiabatic and free from losses. The application of the conventional theory for calculating the losses in the actual flow through a convergent-divergent nozzle of the type considered presents certain difficulties. The theory of what is described as the "losses method" of calculating nozzle efficiency has been presented by Goudie (4, p. 643). The pressure p_1, quality x_1, and total heat h_1 of the steam arriving at the nozzle, and the weight w of the steam flowing per second, are known from the tests. From the readings of the search tube, at any section A_2, the pressure is p_2. At this cross-section the steam is wet but with an unknown quality x_2 since expansion is not perfectly adiabatic. Let V_1 be the small velocity of the steam arriving at the nozzle. If the unknown velocity V_2, at Section 2, is uniform and axial, or nearly so, for all particles, and if y is the friction loss in the nozzle, then the following equation based on the conservation of energy is true (11, p. 68):

$$\frac{V_2^2}{2gJ} = (h_1 - h_2)(1 - y) .$$

The symbol J denotes the mechanical equivalent of heat (1 B.t.u. = 778 ft.-lb.), and h_2 is the total heat in the steam after it has expanded adiabatically to p_2.

The volume discharged at any pressure equals the weight discharged per second multiplied by the specific volume of the steam. The law of steady flow requires that the volume discharged per second equal the area of the section multiplied by the velocity per second. Hence

$$wx_2v_2 = \frac{A_2V_2}{144} .$$

At cross-section A_2 the heat h_2 in the steam is

$$h_2 = x_2h_{fg_2} + h_{f_2}$$

Then the velocity equation becomes

$$V_2 = 173.97 - \left[\frac{A_2h_{fg_2}}{wv_2} + \sqrt{\left(\frac{A_2h_{fg_2}}{wv_2}\right)^2 + 1.6554\,(h_1 - h_{f_2})}\right].$$

In reality, V_2 may not be uniform or axial, x_2v_2 may vary, the amount of variation depending on the distribution of the water drops, and the section may not be filled if the steam leaves the walls. Notwithstanding these difficulties it was expedient to calculate the losses in the brass nozzles Nos. 12, 13, 14, and 15, with a view to comparing the behaviour of the steam in the various forms of nozzle and to account at least in part for the effects of certain recompression phenomena that have been observed.

Nozzle No. 12 will first be considered, and, on the assumption of an ideal expansion in which the process is adiabatic, the velocity, V_m, after expansion to absolute pressure p_m is calculated on the basis of the observed pressures and plotted as an ordinate in Fig. 35 against the distance along the axis corresponding in area to the point at which the nozzle would just be filled by the stream in accordance with the continuity equation. Twelve points in the divergent section of the nozzle are considered and a best fitting curve is drawn through the calculated points. Values of the actual velocity V_2 were calculated by means of the velocity equation on the basis of observed pressures and flow tests. These are plotted as ordinates in Fig. 35 at points along the nozzle axis corresponding to the actual area A_2 of the nozzle. The calculations were extended to include the test conditions listed in Table II for back pressures up to and including 24 psi gauge. Similar calculations were carried out for nozzles Nos. 13, 14, and 15.

The results are summarized in Table V, which gives the calculated velocity, V_m, after an assumed adiabatic expansion to absolute pressure p_m, the actual velocity V_2 based on observed pressures and flow tests, and the loss, y, in percentage.

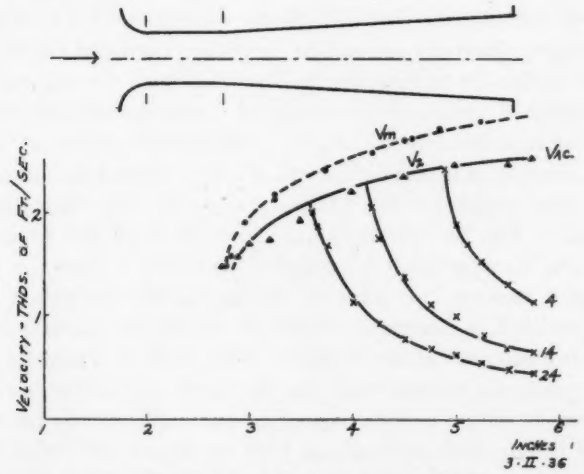

FIG. 35. *Losses in velocity for nozzle No. 12.*

The effect of the nozzle form and its relation to losses and recompression phenomena can now be considered. The greatest loss, 26.6%, is found in nozzle No. 15. This nozzle is characterized by a small ($\frac{1}{4}$ in.) radius of approach, producing a very quick expansion of the steam to throat pressure and a steep pressure expansion curve. The relatively sharp corner of the nozzle, around which the stream must pass, delays the recompression cusp in the curves for the higher back pressures, as, for example, in test No. 14—45/39

TABLE V

CALCULATED VELOCITIES AND LOSSES IN NOZZLES NOS. 12, 13, 14, AND 15

Nozzle No.	V_m Velocity after adiabatic expansion	V_2 Actual velocity	y = loss in per cent of heat drop
12	2940	2530	26
13	2940	2530	26
14	2925	2530	25.2
15	3000	2570	26.6

shown in Fig. 30. A slightly lower recompression pressure, p_r, is produced than in nozzle No. 14 for the same back pressure. The recompression curve following the minimum value p_r is considerably steeper; this denotes a quicker recompression once the process of recompression had begun. The small radius of approach and the sharp corner have produced conditions definitely unfavourable to high efficiency as compared with the larger ($\frac{1}{2}$ in.) radius of approach, more gradual expansion, and best efficiency of nozzle No. 14. The loss in percentage is 26.6 for nozzle No. 15 and 25.2 for nozzle No. 14.

It would appear from the above that, in design, the trend should be toward a larger inlet radius on turbine nozzles than has been the common practice. The introduction of the parallel or extended throat has affected the efficiency adversely both in nozzle Nos. 12 and 13. The parallel throat, in view of later work, is undesirable as it permits growth of water drops, which increase losses. The larger inlet radius of No. 13 has produced a less disturbed pressure expansion curve, Fig. 26, than the small radius of nozzle No. 12, in which the vena contracta recompression is excessive, as shown at point A in Fig. 25. It is concluded that, at this point A, the jet has left the wall of the nozzle. In cases in which it is desired to utilize the nozzle for processing of the jet, such as the introduction at the throat of other fluids at a slightly higher and regulated pressure for mixture with the jet, or the extracting of liquid drops from a vapour jet with a view to improving the quality of the jet, the parallel or extended throat offers advantages both as regards the relatively steady pressure throughout the throat, as noted for nozzle No. 13 in Fig. 26, and the space that may be required for the injection and extraction operations. These advantages may, in such cases, offset the loss of efficiency.

Acknowledgments

The author wishes to acknowledge his indebtedness to Professor A. G. Christie and Associate Professor J. C. Smallwood of the Johns Hopkins University, for their advice and helpful criticism.

References

1. BINNIE, A. M. and WOODS, M. W. Inst. Mech. Eng. Proc. 138 : 229-266; Discussion, 138 : 284-308. 1938.
2. CHRISTIE, A. G. See (12) pp. 427-430. 1934.
3. GOUDIE, W. J. Steam Turbines. London. 1922.
4. GOUDIE, W. J. Ripper's Steam Engine. London. 1932.
5. LEGENDRE, A. M. Nouvelles méthodes pour la détermination des orbites des comètes. Paris. 1806.
6. MARTIN, H. M. Engineering, 95 : 37-38. 1913.
7. MELLANBY, A. L. and KERR, W. J. Roy. Tech. Coll. 1 (Part 2): 123-143. 1925.
8. MELLANBY, A. L. and KERR, W. Trans. Inst. Engrs. & Shipbuilders in Scot. 64. Dec., 1920.
9. POWELL, C. F. Engineering, 127 : 711-713, 779-780. 1927.
10. RETALLIATA, J. T. Am. Soc. Mech. Eng. Trans. 58 : 599-605. 1936.
11. STODOLA, A. Steam and Gas Turbines. McGraw-Hill Book Co., New York. 1927.
12. YELLOTT, JOHN I. Am Soc. Mech. Eng. Trans. 56 : 411-427. Discussion, 427-430. 1934. Or, Engineering, 137 : 303-305, 333-335. 1934.
13. YELLOTT, JOHN I. and HOLLAND, C. K. Engineering, 143 : 647-649. 703-705. 1937.
14. ZERBAN, A. H. and JOHNSTON, R. M. Combustion, 7 : 23-24. 1935.

Canadian Journal of Research

Issued by THE NATIONAL RESEARCH COUNCIL OF CANADA

VOL. 19, SEC. B. JUNE, 1941 NUMBER 6

THE SYSTEM NAPHTHALENE-BENZENE CONSIDERED AS AN IDEAL SOLUTION[1]

BY A. N. CAMPBELL[2]

Abstract

An experimental study of the vapour pressure, and other physical properties, of an ideal system is described. Raoult's law is followed closely by benzene up to high concentrations of naphthalene. Such behaviour may be connected with the smallness of the dipole moments, although that of naphthalene is far from zero. Other physical properties investigated, viz., density, viscosity, and surface tension, show fairly close, but not exact, additive behaviour. In this respect, the behaviour is very similar to that of a system previously investigated, naphthalene–*p*-nitrophenol, where, however, the partial pressures show marked deviation from Raoult's law: this is in harmony with the (presumed) high electric moment of *p*-nitrophenol. It appears, in so far as the two systems studied are concerned, that marked deviation from Raoult's law may be associated with high dipole moment, but that this deviation does not necessarily cause any marked deviation from additivity in other physical properties not dependent on vapour pressure.

Introduction

This work was undertaken as a corollary to previous work on the system naphthalene–*p*-nitrophenol, whose behaviour was shown to be far from ideal (1). The present system was shown by Washburn and Read (6) to exhibit almost ideal behaviour. From the equation

$$d \log N/dT = \Delta H/RT^2$$

they calculated the eutectic temperature as $-3.56°$ C., against an experimental value of $-3.48°$. Using their data, the eutectic composition is calculated as 20.2% naphthalene (benzene separating) and as 21.0% (naphthalene separating), against an experimental value of about 20.2%. There is, therefore, no doubt of the ideal behaviour of this solution. The aim of this work was to exhibit this ideal behaviour in other relations. The physical properties investigated were those listed in the previous paper, with the exception of the properties previously determined by other workers.

Experimental

The heats of fusion of benzene and of naphthalene are known with considerable accuracy (Cf. International Critical Tables). The freezing point diagram has been determined by Pickering (3, pp. 1022 and 1027) and by Lee Ward

[1] *Manuscript received February 5, 1941.*
Contribution from the Department of Chemistry, University of Manitoba, Winnipeg, Man.

[2] *Associate Professor of Chemistry.*

(5, p. 1322), with results in good agreement. The heat of solution of naphthalene in benzene is almost identical with the heat of fusion of naphthalene (4), implying an almost negligible heat of mixing of the liquid components. Gehlhoff (2, p. 254) gives the heat of solution of naphthalene in benzene as -34.5 cal. per gm. (for very weak solutions) as against a heat of fusion of -35.7 cal. per gm. It was therefore not necessary to determine any of the above quantities.

Vapour Pressure

The vapour pressures of solutions of naphthalene in different concentrations in benzene over a range of temperatures were determined by a differential method described in a previous paper (1). This method could be used only up to a content of 60% naphthalene. Beyond this, the method became seriously inaccurate because the preliminary evacuation altered appreciably the concentration of a solution already rich in naphthalene. For solutions richer in naphthalene the expedient of finding the boiling point in an electrically heated Beckmann boiling point apparatus was resorted to, the barometric pressure being followed throughout the experiment.

Vapour Composition

This was not determined directly, but was calculated from the observed total vapour pressure, assuming that naphthalene obeys Raoult's law. The evidence is that in this solution naphthalene does obey Raoult's law, but, even if it deviated considerably, the error involved in the calculation is much smaller than that of any experimental determination.

Density, Viscosity, and Surface Tension

These were determined by the standard methods, mentioned in the previous paper (1), at 79.5° C.

Results

The vapour pressure of pure benzene, in terms of the Clausius-Clapeyron equation, is expressed by the equation

$$\log_{10} p_{mm.} = \frac{-0.05223\,A}{T} + B,$$

where A and B have the values, respectively, 32,295 and 7.6546, for the range 42° to 100° C. (Int. Crit. Tables). To save space, the extensive experimental results for solutions of naphthalene in benzene are expressed in the same form in Table I, by simply reproducing the constants A and B. This table also gives the value of the ratio $\frac{p_{solution}}{p_{benzene}}$ for 80°, which, in terms of Raoult's law, is equal to the mole fraction of benzene, if the partial pressure of naphthalene be neglected, as can be done with the more dilute solutions; the term Δn represents the deviation of this ratio from the mole fraction as calculated from the weight composition. The values of A and B apply to the range of measurement, viz., from the temperature of homogeneity to about 80°.

TABLE I

RESULTS OBTAINED WITH SOLUTIONS OF NAPHTHALENE IN BENZENE

Wt. % naphthalene	Mole fraction of benzene	A	B	p'/p	Δn, %
11.2	0.929	32300	7.6168	0.918	−1.2
24.2	0.8375	31300	7.4006	0.787	−6.1
32.7	0.769	30900	7.3071	0.730	−5.1
43.3	0.683	30500	7.2136	0.692	+1.3
53.8	0.585	33400	7.5921	0.600	+2.6

The value of A is not constant, as perhaps it should be, since it represents essentially the latent heat of evaporation of benzene from solution. If A be constant the observed variations in A then represent the experimental error, viz., about 5%. It is doubtful, however, whether A is really constant, since the temperature coefficient of heat of evaporation may not be the same for solutions of different naphthalene content. Assuming that A is constant at the value of pure benzene (32,295), the figures in Table II are obtained.

TABLE II

VALUES OBTAINED ON THE ASSUMPTION THAT A IS CONSTANT AND EQUAL TO 32,295

Wt. % naphthalene	Mole fraction of benzene	B	p'/p	Δn, %
11.2	0.929	7.6168	0.918	−1.2
24.2	0.8375	7.6006	0.842	+0.9
32.7	0.769	7.5511	0.740	−3.8
43.3	0.683	7.4836	0.643	−6.7
53.8	0.585	7.4321	0.573	−2.0

By the boiling point method, the figures in Table III were obtained.

TABLE III

RESULTS OBTAINED WITH BOILING POINT METHOD

Wt. % naphthalene	Mole fraction of benzene	Boiling point, °C.	P	p'	p	n	Δn, %
50.0	0.620	95.4	738.1	4.9	733.2	0.615	−0.8
60.0	0.523	102.6	745.9	9.2	736.7	0.507	−3.1
70.0	0.413	112.0	742.9	17.9	725.0	0.394	−4.6
80.0	0.293	124.6	741.7	32.7	709.0	0.274	−6.2
90.0	0.155	148.8	738.7	91.4	647.3	0.144	−7.4

NOTE: *P = barometric pressure, p' = partial pressure of naphthalene (calculated from Raoult's law), p = partial pressure of benzene = $P - p'$, $n = \frac{p \text{ benzene in solution}}{p \text{ pure benzene}}$ and Δn = the deviation of this calculated value of mole fraction from that calculated from weight composition.*

On the assumption that the latent heat of evaporation of benzene is constant and equal to 32,295, it is possible to calculate B values from the boiling point experiments, with the results shown in Table IV.

TABLE IV

RESULTS OBTAINED ON ASSUMPTION THAT LATENT HEAT OF BENZENE IS CONSTANT AND EQUAL TO 32,295

Naphthalene, %	50.0	60.0	70.0	80.0	90.0
B	7.4651	7.3673	7.2403	7.0906	6.8311

For the purpose of constructing the complete equilibrium diagram (Fig. 1), the equilibrium temperatures corresponding to the compositions used in the vapour pressure determinations have been read from the plotted data of Pickering (3, pp. 1022 and 1027) and of Ward (5, p. 1322): for these temperatures the vapour pressures, total and partial, have been calculated, as well as the vapour composition.

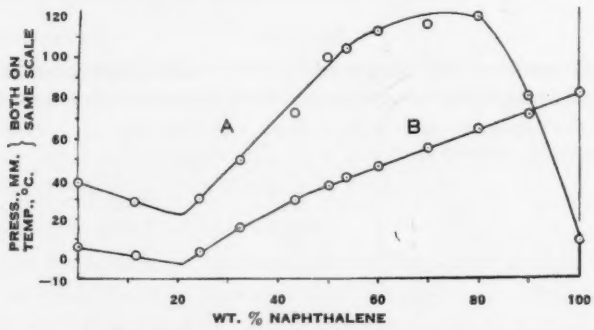

FIG. 1. *Freezing point diagram of system naphthalene-benzene: equilibrium concentrations and pressures. Curve A—vapour pressure; Curve B—equilibrium temperature.*

TABLE V

VAPOUR PRESSURES AND VAPOUR COMPOSITION AT VARIOUS EQUILIBRIUM TEMPERATURES

Wt. % naphthalene	t, °C.	P	p'	p	Per cent naphthalene in vapour
11.2	1.0	27.98	0.00495	27.98	0.0291
24.2	3.0	29.55	0.0112	29.54	0.0618
32.7	15.0	47.99	0.0501	47.94	0.171
43.3	28.0	71.39	0.112	71.28	0.257
50.0	36.0	98.88	0.251	98.63	0.416
53.8	40.0	102.8	0.355	102.4	0.563
60.0	45.0	111.5	0.537	111.0	0.875
70.0	54.0	114.9	1.12	113.8	1.59
80.0	64.0	117.7	2.24	115.5	3.09
90.0	71.0	79.63	3.98	75.6	7.98
100.0	80.0	7.94	7.94	0.0	100.0

The figures obtained for density and molecular volume are contained in Table VI: ΔV represents the deviation from additivity.

TABLE VI

DENSITY AND MOLECULAR VOLUME

Naphthalene, %	$d_4^{79.5°}$	Mol. volume, cc.	ΔV, %
*0.00	0.8154	95.7	—
10.0	0.8267	98.3	+0.39
20.0	0.8390	100.9	+0.57
30.0	0.8551	103.4	+0.39
40.0	0.8738	105.9	+0.05
50.0	0.8896	109.0	−0.02
60.0	0.9076	112.3	−0.16
70.0	0.9236	116.3	−0.03
80.0	0.9424	120.5	−0.12
90.0	0.9598	125.4	−0.06
100.0	0.9779	131.0	—

* *Not determined: taken from International Critical Tables.*

The values of viscosity and surface tension are incorporated in Table VII. The temperature of determination was 79.5° C.

TABLE VII

VISCOSITY AND SURFACE TENSION

Naphthalene, %	Viscosity, poises	S.T., dynes/cm.	Naphthalene, %	Viscosity, poises	S.T., dynes/cm.
0.00	0.00321	—	50.0	0.00520	27.80
10.0	0.00347	22.68	60.0	0.00590	29.20
20.0	0.00385	23.42	70.0	0.00662	30.44
30.0	0.00412	25.00	80.0	0.00765	31.70
40.0	0.00462	26.70	90.0	0.00837	33.00

It was attempted to determine the dielectric constants of solutions of *p*-nitrophenol in benzene with a view to determining the electric moment of *p*-nitrophenol. As a preliminary to this work, the solubility of *p*-nitrophenol in benzene was determined at 30.3° C. It was found to be 2.68 gm. per 100 gm. of benzene. With the available apparatus, however, it was not possible to make the determination of the dielectric constant with accuracy, even in very dilute solution, owing to the high dielectric loss. The mere existence of this dielectric loss, however, is an indication that the dielectric constant and dipole moment of *p*-nitrophenol are high. The dipole moments of benzene and naphthalene are known (8).

Discussion of Results

When the observed values of $\log_{10} 100\,N$ (from the equilibrium figures of Pickering (3, pp. 1022 and 1027) and of Ward (5, p. 1322)) and the values of $\log_{10} 100\,N$ calculated from the ideal equation:—

$$\log_{10} N = \frac{\Delta H}{4.579}\left\{\frac{T_0 - T}{T_0 T}\right\},$$

are plotted against $1000/T$, straight lines of almost identical slope are obtained. The agreement in so far as benzene is concerned is extremely good, indicating that the heat of mixing is zero, or, in other words, that the heat of solution of solid benzene in a solution of benzene in naphthalene equals the heat of fusion of benzene. As regards naphthalene the agreement, though good, shows a small deviation in the sense that the calculated value is almost always slightly lower (maximum deviation at the eutectic = 5.5%) than the observed value. If the calculation is repeated for naphthalene, using instead of the heat of fusion, Gehlhoff's (2) value for the heat of solution, the agreement is better, giving a maximum deviation of 3.5% at the highest concentration of benzene.

Considering the figures for the partial pressures of benzene in solutions of naphthalene in benzene in the light of Raoult's law, it may be said that the deviation from Raoult's law does not exceed 5% up to a concentration of 70% naphthalene, and does not exceed 7.4% at 90.0% naphthalene. The experimental error is assessed as a $\pm 5\%$ (a maximum value), so that the above are limiting values. Probably the actual deviation is less than the limits set. The sign of the deviation is negative, i.e., the observed partial pressure is less than the calculated. For a concentration of 20% naphthalene (benzene solid phase) and an equilibrium temperature of $-3.5°$ C., the vapour pressure of solid benzene is calculated (from the data of the International Critical Tables) to be 18.92 mm., and that of liquid benzene as 21.94 mm., i.e. an apparent mole fraction of 0.860 as compared with 0.8685 from weight composition. This gives a deviation of -0.93%. A similar calculation can be made for the naphthalene side of the diagram, using the data of the International Critical Tables: the constants of the equation for liquid naphthalene were evaluated in the previous paper (1). The constants of this equation have been recalculated as:— $A = 47{,}360$, $B = 7.9012$. When this is done, the deviation from Raoult's law is negligible up to 20% benzene (equilibrium temperature = 64°), but after that increases to an apparent value of about -50% at the eutectic. This figure obviously does not represent the truth, in view of the results of Washburn and Read (6). The discrepancy is almost certainly due to the attempt to apply the Clausius-Clapeyron equation over too great a range (in the case of liquid naphthalene); in other words, the heat of evaporation of liquid naphthalene at a temperature about 80° below the freezing point is not the same as it is above the freezing point. The calculation of Washburn and Read (6) shows that the partial pressure of naphthalene must obey Raoult's law almost equally well with that of benzene.

Little comment is necessary on the density determinations, except to say that there is definitely a slight expansion (mean value = 0.35%) in solutions containing from 0 to 40% naphthalene, which then changes to a slight contraction for higher concentrations of naphthalene (mean value = 0.08%).

International Critical Tables give figures for the viscosity of solutions of naphthalene in benzene at 25° C., of concentrations from 0 to 37.69% naphthalene. When plotted against mole fraction these figures give an almost straight line relation: the fluidity plot has a slight convexity to the axis of concentration. Similar plotting of the experimental results of this paper, for 79.5° C. and the whole range of composition, gives a slight but distinct S-curve: solutions of mole fraction of naphthalene less than 0.55 are less viscous, solutions of mole fraction greater than 0.55 more viscous, than the mixture rule requires. The fluidity curve is smooth with slight convexity towards the axis of concentration.

The curve of surface tension against mole fraction of naphthalene is slightly concave towards the axis of concentration.

According to Williams and Ogg (8), the electric moments of benzene and naphthalene are respectively 0.085 and 0.705. Both values are low, and this is no doubt connected with the ideal behaviour of the solutions. It was found impossible, with the apparatus available, to determine the dipole moment of *p*-nitrophenol experimentally, but it can be calculated with some accuracy. According to Williams (7), the dipole moment of a benzene molecule substituted in the para-position can be calculated additively, provided that the substituents are not too complicated in nature. He gives a table of group moments from which the values are taken:— OH = -1.7×10^{-18} and $NO_2 = -3.9 \times 10^{-18}$. From this, the dipole moment of *p*-nitrophenol results as:— $-1.7 - (-3.9) = 2.2 \times 10^{-18}$. This is an average high value and no doubt accounts for the much greater deviation of the system *p*-nitrophenol–naphthalene from Raoult's law (1).

A general conclusion from the study of only two systems would be unjustifiable, but the following observations may be made:

1. Pronounced deviations from Raoult's law are observed in the system, one of whose components has a high dipole moment.

2. Ideal behaviour is observed in the system, both of whose components have a small dipole moment, one being almost zero.

3. Pronounced deviations from Raoult's law and derived equations are not necessarily associated with marked departure from additivity in regard to other physical properties.

References

1. CAMPBELL, A. N. and CAMPBELL, A. J. R. Can. J. Research, B, 19 : 73-85. 1941.
2. GEHLHOFF, G. Z. physik. Chem. 98 : 252-259. 1921.
3. PICKERING, S. U. J. Chem. Soc. 63 : 998-1027. 1893.
4. TIMOFEJEW, W. Chem. Centr. 76 (2) : 429-438. 1905.
5. WARD, H. L. J. Phys. Chem. 30 : 1316-1333. 1926.
6. WASHBURN, E. W. and READ, J. W. Proc. Nat. Acad. Sci. U.S. 1 : 191-195. 1915.
7. WILLIAMS, J. W. J. Am. Chem. Soc. 50 : 2350-2357. 1928.
8. WILLIAMS, J. W. and OGG, E. F. J. Am. Chem. Soc. 50 : 94-101. 1928.

SYNTHESIS OF 4-HYDROXY-3-METHOXYMANDELAMIDE[1]

By Harry Schwartz[2] and Joseph L. McCarthy[3]

Abstract

4-Hydroxy-3-methoxymandelamide was synthesized from vanillin through the cyanohydrin, the imino ether hydrochloride, and the ethyl ester. Its dibenzoate was prepared from vanillin cyanohydrin dibenzoate by the method of Albert.

The substance 4-hydroxy-3-methoxymandelamide, required as an intermediate in the preparation of hydroxyketones by the Grignard reaction, could not be synthesized directly but was finally prepared, after considerable experimentation as to proper conditions, from vanillin by its conversion successively through vanillin cyanohydrin, the imino ether hydrochloride, and the ethyl ester.

Vanillin cyanohydrin, prepared by the method of Buck (4), was not isolated in crystalline form for the preparation of the imino ether hydrochloride, but was kept in ether solution and the latter treated with ethanol-hydrochloric acid. It was found that when the cyanohydrin is isolated in crystalline form and then treated with ethanol-hydrochloric acid, the yield of the ethyl ester is extremely low (3·5%), presumably owing to decomposition of the cyanohydrin into vanillin and hydrogen cyanide on exposure to the atmosphere.

When the *p*-hydroxyl group of vanillin cyanohydrin is blocked, a substituted derivative of the required amide can be obtained directly. Thus vanillin was treated with potassium cyanide and benzoyl chloride to yield stable vanillin cyanohydrin dibenzoate, a product previously described by Aloy and Rabaut (2). Using the method of Albert (1), the conversion in good yield to the amide dibenzoate was accomplished by refluxing the cyanohydrin derivative with zinc oxide and acetic acid for two hours, instead for one-half hour as recommended by Albert (1). However, the method of Hahn, Stiehl, and Schulz (5) for converting acetyl aryl cyanohydrins of methyl vanillin, isovanillin, and piperonyl into α-chloroacetamides by treatment with anhydrous hydrogen chloride in ether-benzene solution is apparently not applicable to diacetylated vanillin cyanohydrin; this is a good example of the peculiarities encountered in the study of vanillin derivatives as compared with those of other *p*-substituted benzaldehydes (3).

Somewhat surprisingly, neither of the substances, under the conditions employed, could be converted by the Grignard reaction to its corresponding guaiacyl acetyl carbinol derivative.

[1] *Manuscript received in original form November 7, 1940, and as revised, May 8, 1941.*
Contribution from the Division of Industrial and Cellulose Chemistry, McGill University, Montreal, Que.

[2] *Postdoctorate Research Assistant, Division of Industrial and Cellulose Chemistry, McGill University.*

[3] *Sessional Lecturer, McGill University, and holder of a Canada Paper Company Fellowship.*

Experimental

Preparation of Ethyl 4-Hydroxy-3-methoxymandelate

An ether solution (250 cc.) of vanillin cyanohydrin, prepared from 100 gm. of vanillin by the method of Buck (4), was treated with dry ethanol (20 cc.) and anhydrous hydrogen chloride (10 gm.) dissolved in anhydrous ether (50 cc.). On standing overnight at 10° C., the yellowish white salt of the imino ether hydrochloride settled out. The supernatant liquid was decanted off and the salt washed once with anhydrous ether, then hydrolysed as follows: It was dissolved in water (1500 cc.) containing an excess of calcium carbonate, filtered from any insoluble material, made just acid to litmus paper, and then allowed to stand at room temperature for three hours. The solution was then continuously extracted with ether, the ether solution extracted once with saturated sodium bisulphite and twice with saturated sodium bicarbonate solution, dried over calcium chloride, and then the ether was removed under reduced pressure. The residual dark yellow oil was distilled under vacuum. The ester fraction (150 to 170° C. (1 mm.)) was collected, crystallized by scratching, and recrystallized from benzene-petroleum ether. Yield, 25% based on the weight of vanillin taken; m.p., 75 to 77° C.*; mixed m.p. with vanillin cyanohydrin, 55 to 67° C. Found: Alkoxyl (as methoxyl) (6), 26·8%. Calc. for $C_{11}H_{14}O_5$: Alkoxyl (as methoxyl), 27·40%.

Preparation of 4-Hydroxy-3-methoxymandelamide

Ethyl 4-hydroxy-3-methoxymandelate (21 gm.) was dissolved in a minimum amount of ethanol, cooled to 0° C., saturated with anhydrous ammonia gas, and allowed to stand at 0° C. for four days, when the amide (8·6 gm.) settled out. After a further seven days at 0° C., more material (3·2 gm.) separated. Total yield of the amide, 65%. The product was ground in a mortar with ether and recrystallized twice from dioxane-petroleum ether (b.p. 60 to 70° C.) and twice from ethanol; m.p., 136·5 to 137·5° C. Found: C, 54·94; H, 5·83; N (Kjeldahl), 6·9; OCH_3 , 16·0%. Calc. for $C_9H_{11}O_4N$: C, 54·82; H, 5·58; N, 7·1; OCH_3 , 15·76%.

Preparation of 4-Hydroxy-3-methoxymandelamide Dibenzoate

To vanillin cyanohydrin dibenzoate (2 gm., m.p. 145 to 146·5° C.), prepared in 23% yield by the method of Aloy and Rabaut (2), was added zinc oxide (1 gm.), glacial acetic acid (10 cc.), and water (2 cc.), and the mixture refluxed for two hours. The solution was poured into water (250 cc.), and the resulting precipitate was filtered off and recrystallized from ethanol. Yield, 80%; m.p., 176·5 to 177·5° C. Found: OCH_3, 7·8; N (Kjeldahl), 3·40%. Calc. for $C_{23}H_{19}O_6N$: OCH_3 , 7·71; N, 3·45%.

Action of Methyl Magnesium Iodide on 4-Hydroxy-3-methoxymandelamide and its Dibenzoate

4-Hydroxy-3-methoxymandelamide dibenzoate (1 mole) in benzene suspension was added to an ether solution of methyl magnesium iodide (4 moles),

* *Melting points are uncorrected.*

and the suspension refluxed for five hours. Ten per cent sulphuric acid was added, the aqueous layer extracted with ether, and the latter then combined with the benzene layer. This ether-benzene solution yielded a sodium bicarbonate fraction from which benzoic acid was isolated and identified. On evaporation of the residual solution to dryness, there was obtained a dark coloured oil, which did not yield the desired ketone fraction on distillation. When free 4-hydroxy-3-methoxymandelamide was treated with methyl magnesium iodide (using a 5 to 1 ratio of Grignard reagent to amide) and the reaction mixture examined in the same way as described for the dibenzoylated amide, again the expected ketone was not obtained.

Acknowledgment

The authors appreciate the advice and encouragement given by Prof. Harold Hibbert of McGill University.

References

1. ALBERT, A. Ber. 49 : 1382-1385. 1916.
2. ALOY, J. and RABAUT, C. Bull. soc. chim. 11 : 389-393. 1912.
3. BRICKMAN, L., HAWKINS, W. L., and HIBBERT, H. Can. J. Research, B, 19 : 24-33. 1941.
4. BUCK, J. S. J. Am. Chem. Soc. 55 : 3388-3390. 1933.
5. HAHN, G., STIEHL, K., and SCHULZ, H. J. Ber. 72 : 1291-1301. 1939.
6. VIEBÖCK, F. and SCHWAPPACH, A. Ber. 63 : 2818-2823. 1930.

CANADIAN JOURNAL OF RESEARCH

Notes on the Preparation of Copy

General:—Manuscripts should be typewritten, double spaced, and the original and one copy submitted. Style, arrangement, spelling, and abbreviations should conform to the usage of this Journal. Names of all simple compounds, rather than their formulae, should be used in the text. Greek letters or unusual signs should be written plainly or explained by marginal notes. Superscripts and subscripts must be legible and carefully placed. Manuscripts should be carefully checked before being submitted, to reduce the need for changes after the type has been set. All pages should be numbered.

Abstract:—An abstract of not more than about 200 words, indicating the scope of the work and the principal findings, is required.

Illustrations:—Drawings should be carefully made with India ink on white drawing paper, blue tracing linen, or co-ordinate paper ruled in blue only. Paper ruled in green, yellow, or red should not be used. The principal co-ordinate lines should be ruled in India ink and all lines should be of sufficient thickness to reproduce well. Lettering and numerals should be of such size that they will not be less than one millimetre in height when reproduced in a cut three inches wide. If means for neat lettering are not available, lettering should be indicated in pencil only. All experimental points should be carefully drawn with instruments.

Illustrations need not be more than two or three times the size of the desired reproduction, but the ratio of height to width should conform with that of the type page. Small photographs should be mounted on cardboard and those to be reproduced in groups should be so arranged and mounted. The author's name, title of paper, and figure number should be written on the back of each illustration. Captions should not be written on the illustrations, but typed on a separate page of the manuscript.

Tables:—Titles should be given for all tables, which should be numbered in Roman numerals. Column heads should be brief and textual matter in tables confined to a minimum.

References should be listed alphabetically by authors' names, numbered in that order, and placed at the end of the paper. The form of literature citation should be that used in this Journal and titles of papers should not be given. All citations should be checked with the original articles

The *Canadian Journal of Research* conforms in general with the practice outlined in the *Canadian Government Editorial Style Manual*, published by the Department of Public Printing and Stationery, Ottawa.